Solid State Phenomena
ISSN: 1662-9779, Vol. 314, pp 150-154

Submitted: 2020-05-06
Revised: 2020-06-19
Accepted: 2020-06-19
Online: 2021-02-09

Characterization of Wetting of Deep Silica Nanoholes by Aqueous Solutions Using ATR-FTIR

Guy Vereecke[1,a], Audrey Darcos[2], Hideaki Iino[3], Frank Holsteyns[1], and Efrain Altamirano Sanchez[1]

[1]imec, Kapeldreef 75, 3001 Leuven, Belgium

[2]INSA, 26 avenue de Lespinet, 31400 Toulouse, France

[3]Kurita Water Industries Ltd., 1-1, Kawada, Nogi-machi, Shimotsuga-gun, Tochigi, 329-0105, Japan

[a]guy.vereecke@imec.be

Keywords: wetting, nano-confinement, water structuring, contact cleaning, via cleaning

Abstract. In advanced semiconductor manufacturing, deep hydrophilic nanoholes are found in various applications, which require a wet clean after patterning. In this work, we use an in-situ ATR-FTIR spectroscopy technique to characterize the wetting of nanoholes in a silica matrix by UPW and electrolyte solutions. Wetting was much slower than predicted by a numerical model, while temperature cycling evidenced the formation of unexpectedly stable gas pockets in the wetted nanoholes. Water structuring in the nanoholes was characterized by an analysis of the OH stretching peak. Besides, monitoring the dissolution of CO_2 in the wetted nanoholes allowed to compare the diffusivity in the nano-confined solutions with that in bulk solutions. Our results strongly suggest that the gas pockets were stabilized by the decreased gas diffusivity resulting from water structuring.

Introduction

In advanced semiconductor manufacturing, deep hydrophilic nanoholes are found in various applications, which require a wet clean after patterning. For example: (1) nanoholes at the cross points of the gate and channel lines in the RMG module of FinFETs, (2) supervias from M3 to M1 to achieve the required area scaling in the BEOL of the 3 nm node, and (3) deep contact holes with an aspect ratio higher than 60 in 3D-NAND memory multilayers [1-3]. A numerical model predicted a nearly instantaneous wetting of nanoscale features, where wetting is controlled by the diffusion of trapped air outside the cavities [4]. While the wetting of micron-wide 1-D nanotrenches could be studied optically [5, 6], the study of wetting of nanoscale features encountered in semiconductor manufacturing is hampered by their 2-D nanoconfinement. Recently however, an acoustic reflectometry method was used to study wetting of nanoscale deep trench isolation structures, showing uncomplete wetting not only by water, but also mixtures of water and ethanol [7].

In this work, we use an in-situ ATR-FTIR spectroscopy technique [8] to characterize the wetting of nanoholes embedded in a silica matrix by UPW and electrolyte solutions. Wetting was much slower than predicted by a numerical model, while temperature cycling evidenced the formation of unexpectedly stable gas pockets in the wetted nanoholes. Water structuring in the nanoholes was characterized by an analysis of the OH stretching peak. Besides, monitoring the dissolution of CO_2 in the wetted nanoholes allowed to compare the diffusivity in the nano-confined solutions with that in bulk solutions. Our results strongly suggest that gas pockets in nanoholes were stabilized by the decreased gas diffusivity resulting from water structuring.

Materials and Methods

Structures. Dense arrays of silicon nanoholes in a PEALD SiO_2 matrix (depth of about 300 nm, diameter of about 20 nm, and pitch 90 nm, Fig. 1) were fabricated on Si wafers using arrays of nanopillars as sacrificial template, as described in previous work [9].

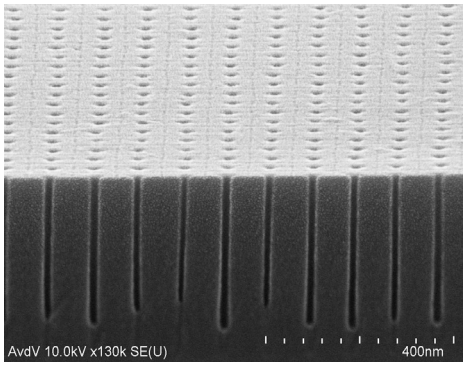

Figure 1: Nanoholes test structure: nanoholes in a PEALD SiO2 matrix on a Si wafer, with depth ~ 300 nm, CD ~ 20 nm, volume ~7 %.

ATR-FTIR. A Nicolet 6700 FT-IR spectrometer (Thermoelectron Corporation) equipped with a liquid nitrogen cooled mercury-cadmium-telluride detector and a customized flow cell was used in the experiments. ATR-crystals were prepared from the patterned wafers by mechanical polishing of slanted windows and were placed as the base plate in the liquid flow cell. More details can be found in [8, 10]. In this setup, the Si crystal acted as a waveguide for the IR beam and total reflection occurred at the Si/SiO_2 interface, with the evanescent wave sensing the nanoholes in the oxide layer. All wetting tests were performed in static mode. As shown by Spuller et al. [4], the diameter of the nanoholes was too small for a liquid flow or convection to play any role in the wetting kinetics. The ATR crystals were dried on a hot plate at 200 °C before mounting in the flow cell. Wetting was characterized by the OH stretching to OH bending peak ratio [8]. This method results from the deeper penetration depth of the evanescent wave at lower frequency (OH bending peak), as opposed to higher frequencies (OH stretching peak). This dependency renders the OH stretching peak more sensitive to the wetting of nanoholes as compared to the OH bending peak. The extent of water structuring was characterized by changes of the OH stretching peak shape as compared to a water reference spectrum obtained on a flat Si crystal [11].

Structure breaking and making salts. In semiconductor manufacturing, solutions for cleaning and etching are often made out of concentrated mineral acids or bases, such as HF or NH_4OH, that are dissociating in reactant ions. According to Marcus [12], ions in bulk aqueous solutions can be classified either as structure making or breaking. In a previous study, we have verified the validity of this classification for solutions wetting nanochannels with a CD of 20 nm and found a good agreement [13]. For example, using salts of Na^+, a borderline ion in Marcus classification, the ranking of structure breaking ions $I^- > Br^- > Cl^- > SO_4^{2-}$ gave $Br^- > I^- > Cl^- > SO_4^{2-}$ in nanochannels. On the other hand, using Cl^- salts, the net structure breaking effect of Cl^- was found secondary, and the ranking of structure making ions $Fe^{2+} > Co^{2+} > Ca^{2+}$ was confirmed in nanochannels. In the present study, NaI and $CoCl_2$ were used as structure breaking and making salts, respectively.

Results and Discussion

Figure 2(a) shows the typical time evolution of the OH stretching/bending area ratio upon wetting and subsequent heating of nanoholes, as a function of the set temperature. As expected, the ratio is found to increase and reach a plateau upon wetting (step 1). This initial wetting was performed at 30 ˚C. The small kink in the wetting curve at a ratio of about 16 corresponds to the wetting of the top surface of the nanoholes array. In a second step, the substrate was heated by increments of 10 ˚C up to the set temperature of 90 ˚C. Each temperature step lasted 10 min. Measurements with a thermocouple indicated that the final surface temperature was about 10 ˚C lower compared to the set point of 90 ˚C. The decrease of the peak ratio upon heating can be attributed to the decrease of water density. In a third final step, the sample was left to naturally cool down back to 30 ˚C, which took about 20 min. The final peak ratio was higher compared to the ratio obtained after the initial wetting step, indicating that wetting of the nanoholes was not complete before performing the heating cycle. In comparison to the predicted short lifetime of nanobubbles [14], on the order of 0.1 ms for a diameter of 100 nm, the gas pockets formed upon wetting had a surprisingly long lifetime that was exceeding 1 hour. Figure 2(b) shows the OH stretching peaks obtained during the heating step at the

various plateau temperatures as compared to the spectrum of bulk water wetting the flat top surface. All peaks were normalized with respect to area for comparison purpose. At 30 ˚C the differences in shape were attributed to water structuring, which was mainly characterized by an increase of absorbance at low wavenumber (read frequency) at the expense of a decrease at high frequency [11]. Upon heating, the peaks at 3200-3400 cm^{-1} were further decreasing, with a concomitant increase of the absorbance at 3500-3600 cm^{-1} that is typical for non-H-bonded OH groups [15]. But little change was observed in the band at 2800-3100 cm^{-1} characteristic of water structuring. Hence no transition to normal, 'destructured', water was observed upon heating in this experiment. Note the decrease of the absorbance at about 3700 cm^{-1}, which can be attributed to the disappearance of non-H-bonded surface OH groups of silanols [15], in agreement with the further wetting of the nanoholes upon heating. The observation that this decrease was larger compared to the initial decrease at 30˚C indicated that the gas pockets were mostly located at the bottom of the nanoholes, where the response to the IR evanescent wave is larger. Likewise, the increase in absorbance at about 3650 cm^{-1} may be attributed to surface silanol groups bonding to water molecules [15].

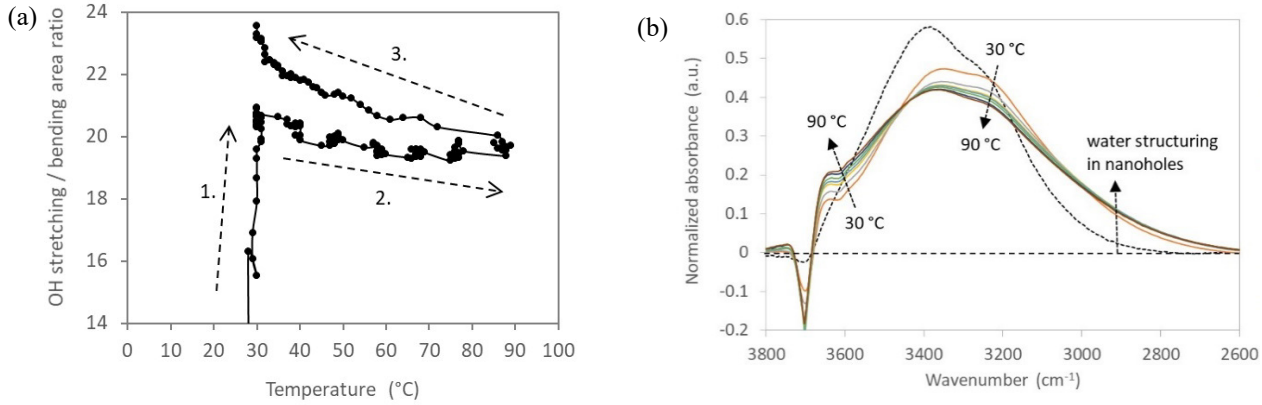

Figure 2: Wetting of nanoholes by UPW and subsequent heating: (a) time evolution of the OH stretching/bending area ratio as a function of the set temperature: 1. wetting at 30 °C; 2. stepwise heating to 90 °C; 3. cooling down to 30 °C; (b) changes in the OH stretching band as a function of wetting and heating; peaks were normalized with respect to area for comparison purpose; the dashed line gives the peak of bulk water on top of the nanoholes as reference.

The wetting time of nanoholes was determined for various solutions at room temperature and for UPW at various temperatures. Figure 3 gives the times measured to reach 90 and 99 % of the plateau in the time evolution of the OH stretching peak area. In general, the wetting time was quite long, on the order of several minutes, as compared to typical times used in wafer processing and to predictions of less than 1 ms from a numerical model [4]. A striking result was the large variability of the wetting times, which was most likely reflecting the variability in the formation of gas pockets. It was too large to reveal any significant effect from the addition of structure making or breaking salts. On the other hand, heating up the substrate helped in decreasing the wetting time, albeit to values still too long for manufacturing. In this respect it is important to note that the solutions were not heated before injection, opening the possibility to decreasing further the wetting time.

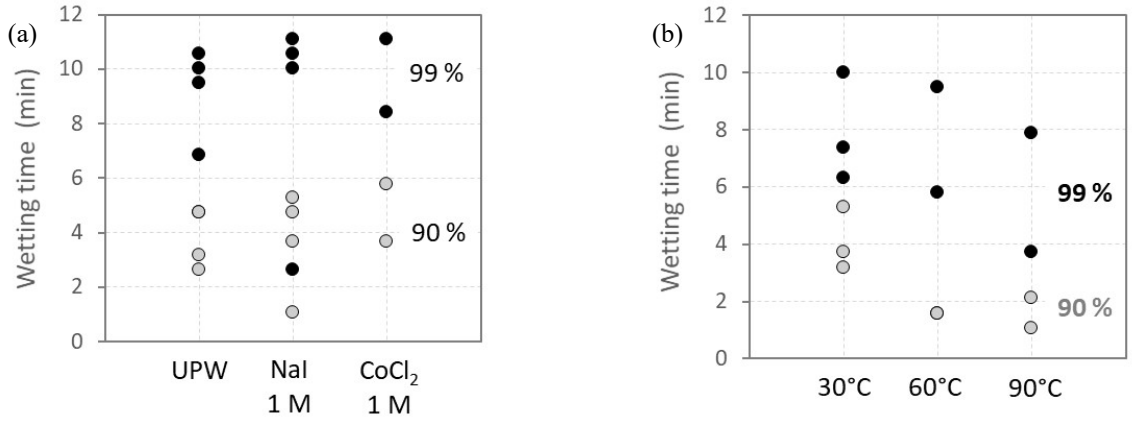

Figure 3: Wetting times of nanoholes for (a) various solutions at room temperature and (b) UPW at various temperatures. Wetting was characterized by the time needed to reach 90 and 99 % of the plateau in the time evolution of the OH stretching peak area.

Finally, the diffusivity in the solutions confined in the nanoholes was characterized using CO_2 gas as a probe. In this purpose, the ATR crystal was first wetted by the solution before being exposed to a CO_2 gas flow at 1 atm in the liquid cell. The solution volume was 5 mL, making a layer of 4.3 mm thickness on top of the crystal. The absorption of CO_2 in the solution was monitored using the C=O stretching peak at about 2350 cm^{-1}. The comparison of the CO_2 peak area from various tests was performed after a normalization based on the area of the respective OH stretching peak. Figure 4 shows the evolution of the normalized CO_2 peak area as a function of the CO_2 gas flow time for nanoholes wetted by various solutions, as compared to the absorption in UPW on a flat crystal, which is representative for diffusion in a bulk solution. In general, the diffusion of CO_2 in the nanoholes was much slower and the solubility was much higher compared to those in bulk solution. The decrease in diffusivity agrees well with the term 'ice-like' sometimes given to structured water [16] and the lower diffusivity of CO_2 in ice. While the increase in solubility agrees well with the lower permittivity reported for structured water in nanotrenches [17] and the rather hydrophobic nature of CO_2 gas. Equilibrium was reached only in the case of the 1 M NaI solution, which took about 2 hours as opposed to about 30 min for the 4.3 mm thick bulk solution. The dissolution of salts seemed to modulate these effects in agreement with their structure-making or -breaking behavior. The

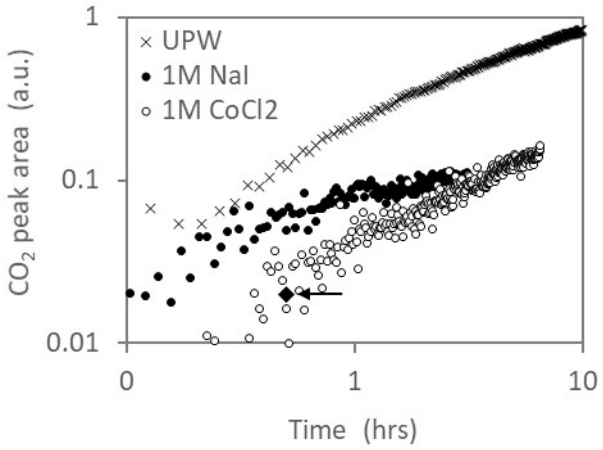

Figure 4: Absorption of CO_2 gas molecules in nanoholes filled with various solutions as a function of the CO_2 gas flow time. The black diamond outlined by an arrow gives the equilibrium level for the absorption in UPW on a flat crystal.

dissolution of NaI led to a relatively faster obtention of equilibrium in about 2 hours and at a lower level, while CO_2 dissolution was slower in presence of $CoCl_2$ and equilibrium had not been reached after about 7 hours. Noteworthy, while improving the diffusion kinetics, the addition of the structure breaking salt could not completely suppress the effect of water structuring. A slower diffusion is

expected to affect not only the chemical reactions performed in cleaning and etching applications, but also the rinsing thereafter. It is most likely also the cause of the surprisingly long life time of the gas pockets formed upon wetting of the nanoholes.

Conclusions

Gas pockets were shown to form upon wetting of 300 nm deep hydrophilic silica nanoholes of a diameter of about 20 nm with UPW and aqueous ionic solutions. This was accompanied by water structuring and a much-decreased gas diffusivity, which was most likely stabilizing the gas pockets against dissolution. The wetting time decreased significantly by heating the solution, while the addition of NaI or $CoCl_2$ at 1 M concentration, respectively a structure making or breaking salt, had no significant effect at room temperature. It is expected that both cleaning and rinsing will also be negatively impacted by the decreased diffusivity.

References

[1] L.-A. Ragnarsson, H. Dekkers, T. Schram, S.A. Chew, B. Parvais, M. Dehan, K. Devriendt, Z. Tao, F. Sebaai, et al., VLSI Tech. Digest (2015) 148–149.

[2] V. Vega-Gonzalez, C.J. Wilson, D. Briggs, et al., IEDM Tech. Digest (2019) 454-457.

[3] S. S.-W. Wang, Semiconductor Eng. (2019), https://semiengineering.com/3d-nand-challenges-beyond-96-layer-memory-arrays/

[4] M.T. Spuller and D.W. Hess, J. Electrochem. Soc. 150 (2003) G476-G480.

[5] J. Haneveld, N.R. Tas, N. Brunets, H.V. Jansen, and M. Elwenspoek, J. Appl. Phys. 104 (2008) 014309.

[6] V.N. Phan, N.-T. Nguyen, C. Yang, P. Joseph, L. Djeghlaf, D. Bourrier, and A.-M. Gue, Langmuir 26 (2010) 13251-13255.

[7] C. Virgilio, L. Broussous, P. Garnier, J. Carlier, P. Campistron, V. Thomy, M. Toubal, P. Besson, L. Gabette, and B. Nongaillard, Solid State Phenom. 255 (2016) 129-135.

[8] N. Vrancken; J. Li, S. Sergeant; G. Vereecke; G. Doumen; F. Holsteyns; H. Terryn; S. De Gendt and X. Xu, Langmuir 33 (2016) 3601-3609.

[9] G. Vereecke, H. De Coster, S. Van Alphen, P. Carolan, H. Bender, K. Willems, L.-Å. Ragnarsson, P. Van Dorpe, N. Horiguchi, and F. Holsteyns, Microelec. Eng. 200 (2018) 56–61.

[10] G. Vereecke, XiuMei Xu, W.K. Tsai, Hui Yang, S. Armini, T. Delande, G. Doumen, F. Kentie, Xiaoping Shi, I. Simms, K. Nafus, F. Holsteyns, H. Struyf, and S. De Gendt, ECS J. Solid State Sci. Technol. 3 (2014) N3095-N3100.

[11] G. Vereecke, H. Debruyn, Q. De Keyzer, R. Vos, A. Dutta and F. Holsteyns, Solid State Phenomena 282 (2018), 182-189.

[12] I. Marcus, Chem. Rev. 109 (2009) 1346-1370.

[13] G. Vereecke, World Chemistry Forum 2019, Forum 2-1: Nanochemistry, Barcelona, Spain, May 22-24, 2019.

[14] S. Ljunggren and J.C. Eriksson, Colloids Surf. A 129-130 (1997) 151-155.

[15] S.L. Warring, D.A. Beattie, and A.J. McQuillan, Langmuir 32 (2016) 1568-1576.

[16] K. Mawatari, Y. Kazoe, H. Shimizu, Y. Pihosh, and T. Kitamori, Anal. Chem. 86 (2014) 4068-4077.

[17] K. Morikawa, Y. Kazoe, K. Mawatari, T. Tsukahara, and T. Kitamori, Anal. Chem. 87 (2015) 1475-1479.